Arabian Journal for Science and Engineering
https://doi.org/10.1007/s13369-026-11224-y

RESEARCH ARTICLE-MECHANICAL ENGINEERING

# Data-Driven Prediction of Wave Energy Potential in the Black Sea Using Ensemble Learning and Real-Time Buoy Observations

Duygu Saydam Irim[1] · Murat Sarıkaya[2] · Salih Dağli[2]

Received: 16 August 2025 / Accepted: 2 March 2026


**Abstract**

This study proposes a machine learning-based framework for short- to medium-term (1–72 h) wave energy forecasting using buoy-measured wave parameters collected from Samsun and Ordu buoys in the Black Sea. Multiple machine learning (ML) techniques, including Long Short-Term Memory (LSTM), Extreme Learning Machine (ELM), Support Vector Machine (SVM), Bayesian Regression, Residual Neural Networks (ResNet), and Recurrent Neural Networks (RNN), were implemented to estimate wave power using forecasted wave parameters. Each model produced independent predictions, which were then integrated through a stacking ensemble approach based on Extreme Gradient Boosting (XGB) to obtain the final wave energy estimates. When compared individually, the ensemble framework provided noticeably lower error levels across all performance indicators, including RMSE, MAE, and MSE, and achieved higher coefficients of determination. Among the tested approaches, the XGB-based ensemble showed mostly reliable performance, particularly for short-term forecasts. For one-hour-ahead predictions, RMSE values were generally between 0.01 and 0.02 m, while $R^2$ values were consistently above 0.99. Although prediction accuracy gradually decreased for longer horizons, the model remained stable for lead times of up to 72 h. Differences were also observed between buoy locations. Predictions derived from the Samsun buoy were more stable than those from Ordu, which is likely related to local variability in wave conditions. Our findings suggested that site-specific dynamics play an important role in wave energy forecasting. Overall, this work demonstrates the potential of combining real-time buoy measurements with ensemble machine learning to estimate wave energy in the Black Sea, providing a practical alternative to computationally intensive numerical wave models and supporting future offshore energy planning.

**Keywords** Wave energy prediction · Black sea · Real-time buoy data · Ensemble machine learning · Energy forecasting · Extreme gradient boosting · Renewable energy integration

## Abbreviations

| | |
|---|---|
| ANN | Artificial neural network |
| ELM | Extreme learning machine |
| LSTM | Long short-term memory |
| SVM | Support vector machine |
| XGB | Extreme gradient boosting |
| ML | Machine learning |
| RMSE | Root mean square error |
| MAE | Mean absolute error |
| MSE | Mean squared error |
| $R^2$ | Coefficient of determination |
| $H_s$ | Significant wave height (m) |
| $T_e$ | Wave period (s) |
| $P_w$ | Wave power (kW/m) |

✉ Murat Sarıkaya
msarikaya@sinop.edu.tr

Duygu Saydam Irim
duygusaydam.ds@gmail.com

Salih Dağli
sdagli@sinop.edu.tr

[1] Institute of Graduate Programs, Sinop University, Sinop, Türkiye

[2] Department of Mechanical Engineering, Sinop University, Sinop, Türkiye

## 1 Introduction

Energy plays a central role in national development, shaping economic growth, industrial activity, and overall quality of life [1]. Over the past few decades, global energy demand

Published online: 27 March 2026

has continued to rise, driven largely by population increase, rapid urbanization, and expanding technological use [1]. This growing demand has also led to a heavier dependence on fossil fuels. While these resources have supported development, their widespread use has brought serious environmental consequences, particularly in the form of climate change and global warming [2]. For this reason, there has been a strong and growing interest in shifting toward cleaner and more sustainable energy sources [3].

Among the various renewable energy options, including solar, wind, geothermal, biomass, hydropower, hydrogen, and marine energy, wave energy has attracted increasing attention in recent years [4, 5]. One of its main advantages is that it provides a relatively dense and more predictable source of energy compared to many other renewables, while at the same time having a comparatively low environmental footprint [6]. Given that oceans cover nearly 70% of the Earth's surface, a large portion of the global wave energy potential remains largely unexplored [7].

Nevertheless, the commercial deployment of wave energy converter (WEC) systems is still at a relatively early stage. A major difficulty arises from the highly variable nature of ocean waves, which makes both steady power generation and grid integration more challenging [8, 9]. For this reason, reliable forecasts of site-specific wave characteristics—such as significant wave height, wave period, and wave direction—are critically important for optimizing system performance and estimating energy output [10]. These parameters, which are commonly derived from buoy measurements, also play a key role in evaluating mechanical stresses and maintaining the structural safety of WEC installations.

Moreover, wave forecasts are important not only for energy applications but also for areas such as coastal structure design and disaster risk reduction [11]. Over time, many different forecasting approaches have been developed, including statistical methods, numerical models, and more recent soft-computing and hybrid techniques. Among these, numerical wave models are based on the physical laws that describe wave motion and ocean–atmosphere interactions. They make it possible to simulate wave conditions over large spatial domains and long time periods using equations derived from fluid dynamics and meteorology. Well-known models such as Wave Model (WAM) [12], Simulating WAves Nearshore (SWAN) [13], and WaveWatch III (WW3) [14] are widely used in coastal engineering and have also been applied to improve the design and performance of wave energy conversion systems.

Wave forecasting and wave energy estimation have been widely studied using a range of different methodologies. Depending on the purpose of the study and the required forecasting horizon, researchers have applied physics-based numerical models, statistical techniques, as well as machine learning approaches. Each of these methods offers certain strengths, but also comes with limitations related to data availability, computational demand, prediction accuracy, and suitability for real-time applications. For this reason, many recent studies compare different techniques to identify the most appropriate solution for a given problem. In this study, a summary of the most used wave forecasting approaches reported in the literature is provided in Table 1.

Physics-based models are well-suited for long-term climate analyses; however, their high computational cost and reliance on external meteorological inputs limit their applicability in real-time and location-specific forecasting. By contrast, machine learning-based methods are able to generate fast and site-specific predictions directly from buoy observations. In addition, ensemble and stacking techniques often lead to better forecasting results by compensating for the weaknesses of individual models and increasing overall accuracy. Within this framework, the present study seeks to fill an important gap in the literature by developing an operational approach for short- and medium-term wave energy forecasting that combines real-time buoy data with multiple regression models through a stacking strategy.

On a global scale, the highest wave energy levels are typically found in the mid-latitude belts between 40° and 60° in both the Northern and Southern Hemispheres, where strong and persistent westerly winds dominate. Previous studies have reported substantial wave power potential in several of these high-energy regions, including approximately 574 GW along the Australian coastline and about 324 GW off the west coast of South America [19]. The geographical location of the Black Sea is illustrated in Fig. 2b, where the region is highlighted in blue and the corresponding latitude bands are shown on the left axis. As indicated in the figure, the study area falls within the 40°–60° N mid-latitude zone, which is commonly considered favorable for wave and other marine renewable energy applications.

Although ocean energy technologies (including wave and tidal) are still under development, the total global installed capacity of ocean power has gradually increased, reaching roughly 500 MW by the end of 2024. A large share of this capacity comes from established tidal barrage plants such as the Sihwa Lake installation in Korea and the La Rance station in France, which together account for most of the operating capacity worldwide. Wave energy, however, represents only a small fraction of the ocean energy portfolio, with relatively few large-scale grid-connected projects in operation. As a result, commercial-scale deployment of wave energy systems remains limited when compared to more mature renewables like wind and solar, which have installed capacities in the hundreds of gigawatts range. Despite this, gradual growth in pilot and demonstration projects around the world suggests increasing interest and investment in wave energy technologies [20].

**Table 1** Comparison of wave forecasting techniques used in literature

| Method/approach | Input data | Computational cost | Advantages | Limitations |
|---|---|---|---|---|
| *Physics-based models (SWAN, WAM, WW3)* [13] | Wind fields, bathymetry, boundary conditions | High | Physical consistency, suitability for long-term analysis | High computational demand, dependency on external meteorological data |
| *Statistical models (e.g., ARIMA)* [15] | Historical wave data | Low | Simple implementation, fast computation | Linear assumptions, limited prediction accuracy |
| *Single ML models (LSTM, SVM, ANN)* [16] | Buoy measurements | Moderate | Ability to capture nonlinear relationships | Model dependency, limited generalization |
| *Deep learning models (ResNet, LSTM)* [17] | Multivariate time series | Moderate–High | Learning of complex patterns | Long training time, high data demand |
| *Ensemble/stacking methods* [18] | Multiple model outputs | Moderate | Improved accuracy, error reduction | Increased model complexity |
| *This study (ML + stacking + real-time buoy data)* | Real-time buoy measurements | Moderate | Location-specific, fast, high prediction accuracy | Not suitable for long-term climate-scale forecasting |

Although the Black Sea is often considered less energetic than the open oceans, regional studies indicate that several sections of the Turkish coastline have notable wave energy potential, in some cases comparable to the Aegean and Mediterranean coasts [21, 22]. In particular, research focusing on the southeastern Black Sea has identified areas around Sinop, Samsun, and Ordu as especially promising for wave energy development [23]. For example, Akpınar and Kömürcü [12] applied the third-generation SWAN model to evaluate offshore wave energy at seven locations along Turkey's Black Sea shoreline, and their results showed that Sinop exhibits the highest wave power potential among the examined sites.

In addition to physics-based modeling, ML approaches have become increasingly popular for forecasting wave parameters. A wide range of algorithms, including artificial neural networks (ANNs), SVM [24], RNN, ResNet, LSTM [25], and ELM, have been explored for their ability to represent the complex and nonlinear nature of ocean waves [26]. In particular, deep learning architectures such as ResNet [27] and LSTM [17, 28] have achieved strong performance in both short-term and long-term prediction tasks. In parallel, ensemble learning techniques, including XGB [18] have shown promising results by combining the outputs of different base models, such as LSTM [29] and SVM [16] to improve overall forecasting accuracy.

While previous studies have focused largely on the estimation of wave height and period, few have directly addressed how these predictions can be translated into accurate wave energy potential forecasts. This constitutes a significant research gap, especially in relatively underexplored basins like the Black Sea. Additionally, while numerous comparative analyses have evaluated model performance using buoy data across global regions, comprehensive wave power predictions specific to the Turkish Black Sea coast remain scarce.

In response to these gaps, this study proposes a hybrid machine learning framework that integrates multiple regression models for predicting short-to medium-term forecasts (from 1 to 72 h) of wave parameters and ultimately wave energy potential. Utilizing one year of hourly buoy data (2023) from two sites (Samsun and Ordu) provided by the Turkish State Meteorological Service, the study develops separate models for estimating significant wave height and period. These buoy's data are first processed through quality control, missing-data treatment, and normalization steps to ensure that they are suitable for modeling. The cleaned dataset is then split into training and testing sets while maintaining the temporal structure of the time series. Afterward, several base regression models, namely, Bayesian regression, ELM, SVM, RNN, LSTM, and ResNet are used to generate independent predictions of wave parameters for different forecast horizons. These regression models were trained and validated in MATLAB. The outputs from these regression models are combined through a stacking strategy based on an XGB meta-model. The XGB model was trained and validated in Python. The resulting final estimates of wave height and wave period are used to calculate wave energy using analytical equations. In the final step, system performance is evaluated using standard metrics, including MAE, RMSE, MSE, and $R^2$. The overall workflow of the proposed machine learning-based wave energy forecasting framework is presented in Fig. 1.

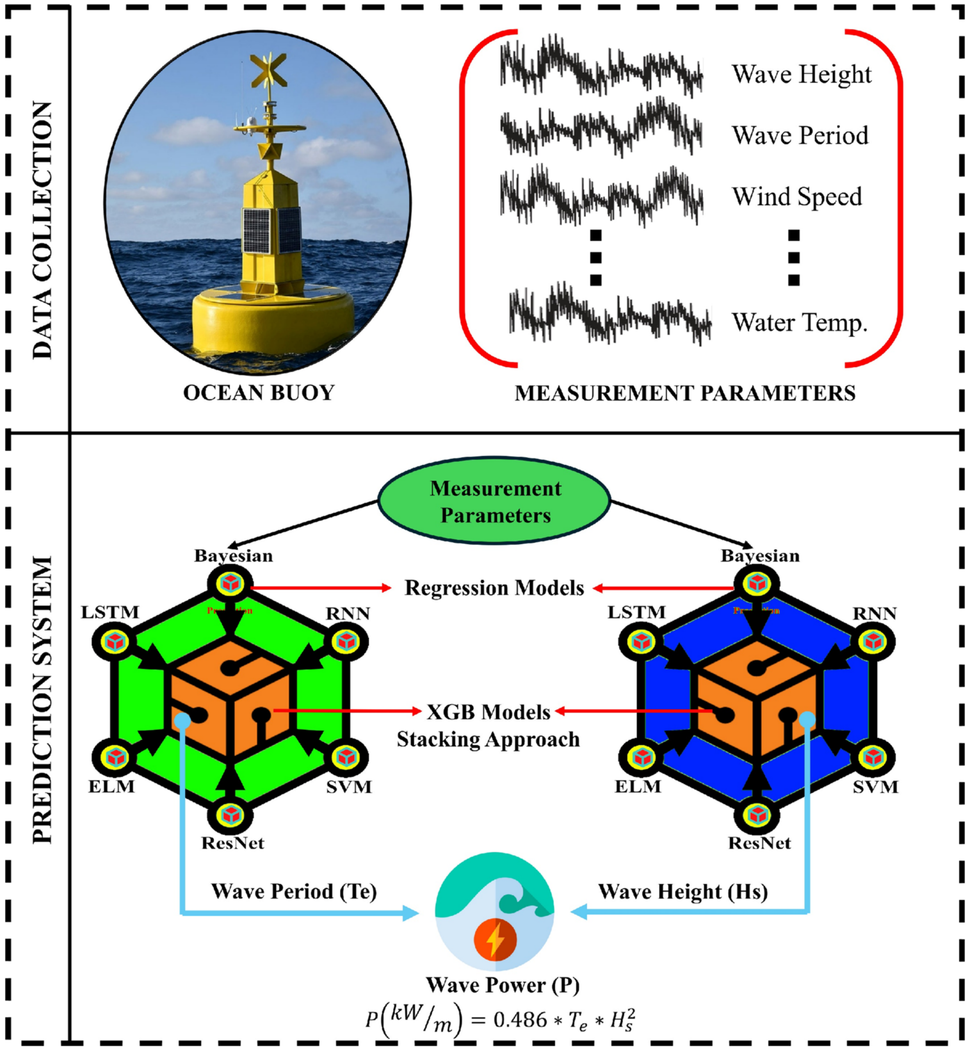


**Fig. 1** Step-by-step workflow of the proposed machine learning-based framework for short- to medium-term wave height, wave period, and wave power prediction

By merging the strengths of diverse algorithms, the proposed framework aims to deliver improved forecasting performance for both short- and medium-term horizons. The proposed approach is designed to support practical decision-making, including daily and weekly energy production planning for WEC systems, maintenance scheduling, and the integration of energy storage. In this context, the developed model structure provides fast, location-specific predictions using only measured buoy data, without requiring the high computational cost or external meteorological inputs typically associated with numerical wave models. Through its focus on the Black Sea which is an underrepresented yet strategically important maritime region, this research seeks to contribute valuable insights to the literature on renewable energy forecasting and inform future WEC system deployments.

## 2 Methodology

This study aims to estimate the potential electrical energy that can be harvested from ocean waves using multiple measurement parameters obtained from marine buoys. The methodological framework consists of three main stages: preprocessing and cleaning of raw buoy data, training of baseline regression models, and the implementation of a stacking-based ensemble approach for forecasting significant wave height and wave period. Subsequently, the potential electrical energy is indirectly calculated using the predicted wave height and wave period values. This structured pipeline enables a systematic evaluation of wave energy potential based on data-driven modeling techniques.

### 2.1 Study area and buoy data

This study utilizes 2023 observational data collected from marine buoys located off the coasts of Ordu and Samsun in the

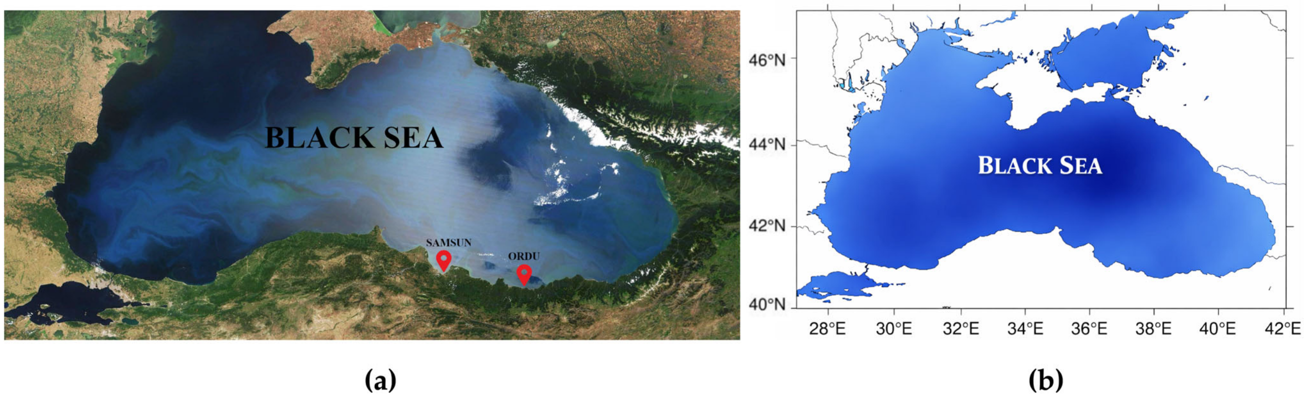


**Fig. 2** **a** Map of the Black Sea showing the locations of the study points, **b** the Black Sea study sites (Ordu and Samsun) latitude band

Black Sea, provided by the Turkish State Meteorological Service (TSMS). The Ordu buoy (ID: 17397) is situated near the Ordu-Giresun Airport at coordinates 41°2′39" N, 38°6′51" E. Similarly, the Samsun buoy (ID: 17391) is positioned in the open waters of Samsun Bay, at 41°26′16" N, 38°33′34" E. Both buoys have a total height of 4.51 m and are equipped with a 1.8-m tower structure, powered by solar energy systems. The locations of the buoys used in this research are illustrated in Fig. 2.

The data used in the study are real measurements taken from buoys deployed at specific locations. The buoys are equipped with different sensors depending on the parameter to be measured. An accelerometer is used to measure wave height. A three-axis accelerometer placed on the buoy detects wave motion. The wave period is calculated by determining the time difference between two consecutive wave crests using a data logger. Other parameters are measured using appropriate sensors. In addition to wave height and peak wave period measurements, several auxiliary environmental variables were monitored through standard meteorological and oceanographic sensors integrated into the buoy system. In this context, wind speed and wind direction were recorded using anemometers, while sea surface conditions were measured via environmental sensors embedded in the buoy platform. As a result, the proposed forecasting framework offers a streamlined and operational data-driven structure based exclusively on measured wave parameters.

The dataset includes a wide range of oceanographic and meteorological parameters measured at varying depths. These parameters are as follows: Current direction at 5 m, 10 m, 15 m, and 20 m depths (in degrees); current speed at 5 m, 10 m, 15 m, and 20 m depths (in cm/s); significant wave height (in meters); maximum wave height (in meters); wave direction (in degrees); mean wave period (in seconds); peak wave period (in seconds); sea surface temperature (°C); air temperature (°C); actual atmospheric pressure (hPa); sea level reduced pressure (hPa); mean wind speed (m/s); maximum wind speed (m/s).

The statistical summary of key parameters measured by both Ordu and Samsun buoys is presented in Table 2. There are cases where the buoys cannot take measurements, such as during maintenance or in the event of a malfunction and are turned off. Although the buoys are identical, they cannot take measurements if they are turned off due to differences in location. In some cases, they can measure temperature but not wave height. Considering the parameters used in model training, complete data sets may differ between buoys. The total number of data records obtained throughout 2023 was approximately 18,000 for the Ordu buoy and 15,000 for the Samsun buoy. These datasets were divided into training (80%) and testing (20%) subsets for use in the design and validation of the predictive models. Temporal variations in significant wave height and peak wave period recorded by the Ordu and Samsun buoys are illustrated in Fig. 3.

The effects of the parameters on wave height and wave period vary. For estimating wave height, the following parameters were used; current speed 5 m (cm/sec.), current speed 10 m (cm/sec.), current speed 15 m (cm/sec.), maximum wave height (m), wave period (sec), mean wind velocity (m/sec), and maximum wind velocity (m/sec) parameters were used. For wave period estimation, the following parameters were used; significant wave height (m), maximum wave height (m), mean wind velocity (m/sec), and maximum wind velocity (m/sec) parameters were used to train the models.

## 2.2 Extreme learning machine (ELM)

The ELM is a learning algorithm designed specifically for single hidden layer feedforward neural networks (SLFNs). Introduced by [30] ELM offers a significant advantage over traditional feedforward neural networks in terms of training speed and generalization performance. Unlike gradient-based methods, ELM randomly assigns the input weights

**Table 2** Summary statistics of selected buoy parameters for Ordu and Samsun (2023)

| Parameter | Ordu Buoy—Mean | Min | Max | Samsun Buoy—Mean | Min | Max |
|---|---|---|---|---|---|---|
| Current speed at 5 m (cm/s) | 17.35 | 0.1 | 383.9 | 17.34 | 0.1 | 723.6 |
| Current speed at 10 m (cm/s) | 23.70 | 0.1 | 453.6 | 18.35 | 0.1 | 686.2 |
| Current speed at 15 m (cm/s) | 26.88 | 0.1 | 387.2 | 18.98 | 0.1 | 633.1 |
| Significant wave height (m) | 0.62 | 0.01 | 3.65 | 0.68 | 0.01 | 3.8 |
| Maximum wave height (m) | 1.00 | 0.01 | 5.58 | 1.11 | 0.01 | 5.96 |
| Wave period (s) | 2.98 | 1.9 | 4.9 | 2.89 | 1.9 | 4.8 |
| Sea surface temperature (°C) | 17.19 | 7.7 | 35.8 | 15.97 | 7.6 | 35.3 |
| Actual pressure (hPa) | 1015.86 | 1000.1 | 1036.6 | 1017.08 | 1000.1 | 1039.7 |
| Sea level reduced pressure (hPa) | 1016.12 | 1000.3 | 1036.9 | 1017.37 | 1000.3 | 1039.9 |
| Mean wind velocity (m/s) | 3.95 | 0.6 | 15.7 | 5.25 | 0.6 | 15.9 |
| Maximum wind velocity (m/s) | 4.96 | 0.7 | 20.4 | 6.39 | 0.8 | 20.9 |

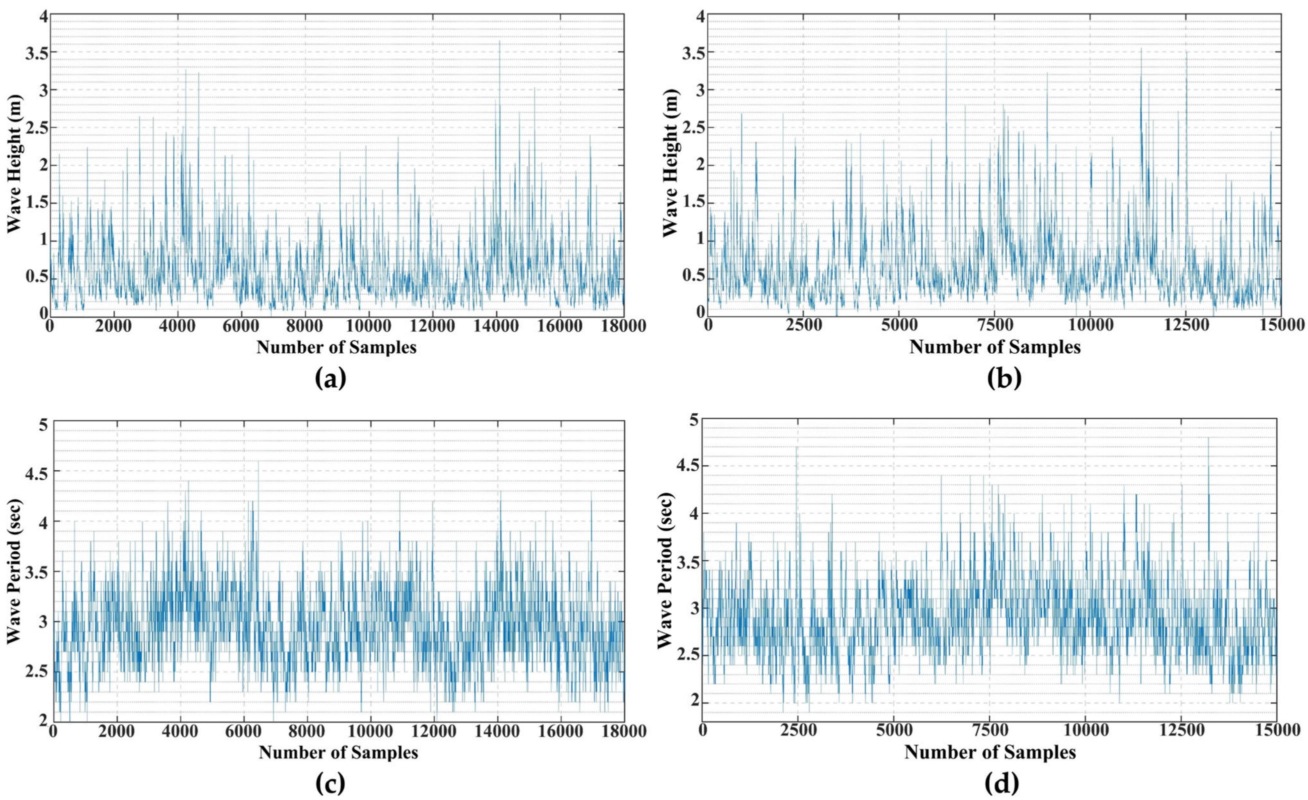


**Fig. 3** **a** Annual time series of significant wave height for Ordu buoy, **b** annual time series of significant wave height for Samsun buoy, **c** annual time series of wave period for Ordu buoy, **d** annual time series of wave period for Samsun buoy

and hidden layer biases, and determines the output weights analytically, leading to faster learning and reduced computational complexity. The output of an ELM is expressed as a nonlinear transformation of the weighted sum of activation values from the hidden layer nodes:

$$\mathrm{ELM}(x) = g\left(\sum_{j=1}^{L} \beta_J h_j[x] + b_0\right) \tag{1}$$

where $g$ is the activation function; $h_j[x]$, denotes the activation value of the $j$-th hidden neuron for input $x$; and $\beta_J$ represents the output weight associated with the $j$-th hidden neuron.

$$g(z) = \frac{1}{1 + e^{-z}} \tag{2}$$

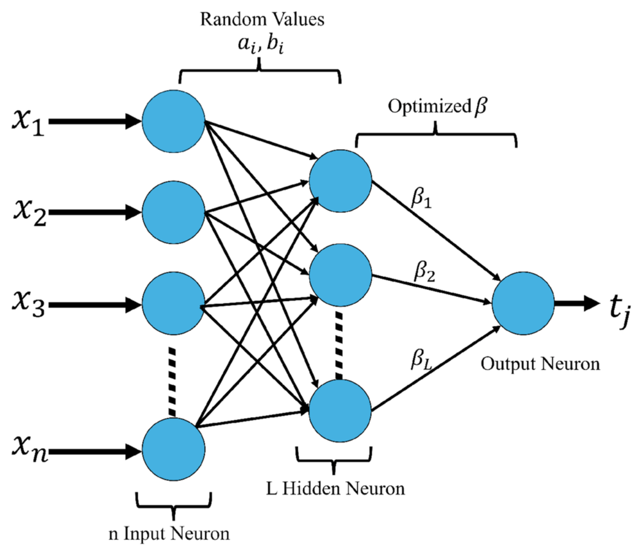


**Fig. 4** Structural representation of the ELM

The activation value $h_i(x)$ of the $i$-th hidden node for an input vector $x \in mathbbR^n$ is calculated as:

$$h_i[x] = g\left(\sum_{j=1}^{n} a_{j,i}x_j + b_j\right) \quad (3)$$

where $a_{j,i}$ are the randomly initialized input weights and $b_j$ denotes the bias term of the hidden node. The general structure and workflow of the ELM algorithm are illustrated in Fig. 4.

### 2.3 Bayesian regression model

Bayesian regression is a probabilistic modeling approach that incorporates prior knowledge or beliefs to generate more reliable predictions from data. It has gained prominence as a robust tool for handling uncertainty and modeling complex relationships in datasets where traditional methods may fall short [31]. By integrating uncertainty directly into the regression framework, Bayesian regression offers a more flexible and informative alternative to classical linear regression, particularly in cases where data is sparse or noisy. The fundamental principle behind Bayesian regression lies in updating prior beliefs about the parameters of a linear model using observed data, through the application of Bayes' Theorem. This approach yields a posterior distribution over model parameters, rather than fixed point estimates, thereby allowing for quantification of uncertainty in predictions.

A Bayesian network which is a key component in this approach is a directed acyclic graph (DAG) consisting of nodes and a set of conditional probability tables (CPTs) defining dependencies between them. Structurally, the network is composed of two primary elements: the topological arrangement of the nodes and the conditional distributions that describe how each node depends on its parents [32]. This probabilistic structure not only supports regression tasks but also proves beneficial for model selection, anomaly detection, and robust handling of outliers. Overall, Bayesian regression enhances predictive performance while offering deeper interpretability in scenarios characterized by uncertainty or variability.

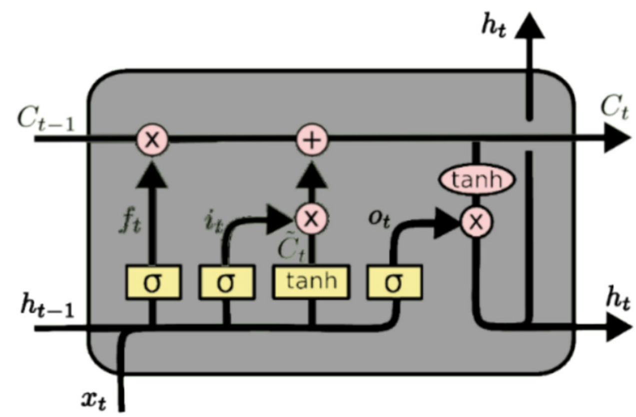


**Fig. 5** Structural diagram of an LSTM cell

### 2.4 Long short-time memory (LSTM)

LSTM is a specialized architecture of RNNs that is particularly effective for modeling long-term dependencies in time series data. Unlike standard RNNs, which tend to struggle with vanishing or exploding gradient problems over long sequences, LSTM networks are designed to remember information over extended periods, making them highly suitable for dynamic, temporal prediction tasks such as wave height forecasting [33, 34].

What distinguishes LSTM from conventional RNNs is its unique memory cell structure, which includes a cell state and a set of gating mechanisms. The cell state acts as a conveyor belt, allowing information to flow unchanged across many time steps unless intentionally modified by these gates. This design helps mitigate the loss of important long-term dependencies, a common issue in time series learning. The architecture of an LSTM unit typically comprises three primary gates. Forget gate: Decides which information should be discarded from the cell state. Input gate: Determines which new information should be added to the cell state. Output gate: Controls which part of the cell state is output as the hidden state at each time step. A visual representation of the LSTM cell structure is provided in Fig. 5, illustrating how these gates interact to manage memory and flow of information.

The horizontal line running across the top of the cell represents the internal cell state, acting as a persistent memory path throughout the sequence. This path allows information to pass through time with minimal modification, thereby preserving context over long sequences. The gating mechanisms (represented as neural network layers within the cell) selectively add or remove information based on its relevance, enhancing the model's capacity to retain critical knowledge over time [35]. Due to these features, LSTM networks are widely used in time-dependent modeling tasks across fields such as oceanography, meteorology, and financial forecasting, where the ability to capture long-term patterns is essential.

### 2.5 Recurrent neural network (RNN)

RNNs offer a flexible and intuitive approach to modeling sequential data by incorporating temporal dependencies through internal recurrence. Unlike feedforward networks, RNNs are equipped with feedback connections that allow information to persist across time steps. This feedback mechanism enables RNNs to detect and learn patterns over time, making them particularly well-suited for tasks involving time series data, such as wave height prediction.

At each time step $t$, the network maintains a hidden state $h_t$, which serves as a memory of previous computations. The output at each step depends not only on the current input but also on the hidden state from the previous time step. This recursive structure allows the network to capture dependencies across different time intervals. Each element of a sequence of length $T$ is processed in an identical manner, with the hidden state carrying forward relevant contextual information [36]. The structural flow of information within a basic RNN unit is illustrated in Fig. 6, highlighting how the hidden state is updated iteratively and passed forward across time steps.

RNNs are designed to operate on ordered input sequences and can utilize historical information to enhance future predictions. This makes them particularly effective in applications involving temporal patterns, such as modeling ocean wave dynamics. In the context of wave height prediction, RNNs are capable of learning from past wave data and capturing the inherent sequential dependencies that influence future wave behavior. Compared to more complex models like LSTM or GRU, standard RNNs have a simpler architecture and typically require less computational effort for training. While they may struggle with long-term dependencies due to vanishing gradient issues, their efficiency and simplicity make them a valuable tool for modeling short- to medium-range temporal patterns. In this study, the RNN model was trained on buoy-derived wave height data to construct a regression model for predicting future wave heights. Its ability to learn from sequential inputs makes it a suitable candidate for this task.

### 2.6 Support vector machine (SVM)

The SVM algorithm, originally proposed by Vapnik [37], employs an ε-insensitive loss function that allows a degree of tolerance for errors within a defined margin. The formulation adopted in this study follows the terminology and approach described by Smola and Schölkopf [38] and Müller et al. [39]. SVM maps the original data points from the input space to a higher-dimensional feature space $F$ using a transformation function $\Phi$. In this transformed space, a linear model is constructed that corresponds to a potentially nonlinear relationship in the original space:

$$\left.\begin{aligned} &\Phi : R^n \to F,\ w \epsilon F \\ &f(x) = \langle w,\ \Phi(x)\rangle + b \end{aligned}\right\} \tag{4}$$

The objective of the ε-insensitive regression is to find a function that approximates the training data with a maximum deviation of ε, while also maintaining the function as flat as possible. This is achieved by minimizing the norm $\|w\|^2$, effectively searching for a small-weight vector that controls the model's complexity.

Wave height prediction is inherently nonlinear and influenced by numerous interrelated meteorological and oceanographic factors, including wind speed, water level, and atmospheric pressure. SVM is well-suited for capturing these complex dependencies, particularly through the use of nonlinear kernel functions. Among them, the Radial Basis Function (RBF) kernel is especially effective in modeling intricate relationships between inputs and outputs, enabling the SVM to deliver high prediction accuracy for wave height estimation. The model's bounded output and ability to avoid extreme overestimations is particularly beneficial for applications involving safety–critical predictions such as wave dynamics. SVMs also excel in multivariate problems, learning from multiple inputs—such as wind speed, air pressure, and water temperature, simultaneously. Their strong generalization capability allows them to perform well on unseen data, reducing the risk of overfitting. Given these strengths, SVM was selected in this study as a suitable machine learning model for wave height prediction. The buoy-derived data were used to train the SVM-based regression model, leveraging its ability to model nonlinear interactions effectively while maintaining robust generalization.

### 2.7 Residual neural network (ResNet)

The key innovation behind ResNet is the introduction of shortcut (or residual) connections that allow the input of a layer to be directly added to the output of a deeper layer. These connections enable efficient gradient flow throughout the network during backpropagation, making it easier

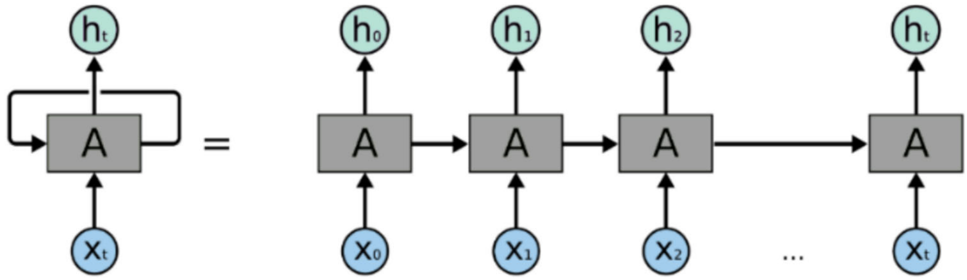


**Fig. 6** Schematic representation of a basic RNN loop

to train very deep architectures. As a result, ResNet allows the construction of deeper networks without suffering from the vanishing gradient problem, leading to more accurate learning, especially when working with large and complex datasets [40]. Originally developed for image recognition tasks, ResNet has also shown strong performance in regression problems by modifying the final layer to produce continuous output values [41]. This makes it a suitable architecture for time series prediction, including applications such as wave height forecasting. Wave height is influenced by a wide range of environmental variables, such as wind speed, water temperature, and atmospheric pressure, all of which interact in nonlinear and complex ways. Accurately modeling these interactions requires deep learning models with high representational capacity. ResNet's structure is well-suited for this purpose, as its residual connections facilitate the training of very deep networks capable of learning intricate dependencies across variables and time steps. Another advantage of ResNet is its ability to capture long-term dependencies in sequential data through deeper architectures, without degrading performance. In wave forecasting tasks, this is particularly beneficial, since past measurements often carry crucial information about future wave behavior. By effectively learning from these long-range patterns, ResNet models can provide more precise and robust predictions.

In this study, ResNet was adopted as a regression model trained on buoy data for wave height prediction. Its ability to handle multivariate inputs and its flexibility in learning complex nonlinear relationships make it a powerful tool for addressing the challenges of modeling ocean dynamics. Furthermore, its strong generalization performance and training efficiency highlight its potential for real-world applications in marine forecasting, especially in scenarios requiring high accuracy across multiple influencing variables [42].

## 2.8 Stacking approaches

Stacking is an ensemble learning technique that combines the strengths of multiple regression models to improve predictive accuracy. In this approach, the original dataset is split into several subsets, which are then used in k-fold cross-validation to train a set of base-level models in the first layer. The predictions generated by these base models are used as input features for a second-level model, often referred to as the meta-model. The meta-model aggregates the outputs of the base regressors, assigning appropriate weights to each prediction to generate the final forecast [43, 44]. This layered architecture enhances overall performance by leveraging the complementary strengths of diverse learning algorithms. However, the accuracy of a stacking model is inherently dependent on the quality and diversity of its base models. Additionally, the number of base models selected has a direct impact on computational efficiency. Therefore, in this study, both prediction performance and training time were considered when selecting the constituent models for the stacking ensemble. The workflow of the stacking approach used in this research is illustrated in Fig. 7.

In this study, the meta-model selected for the stacking approach is the XGB algorithm. XGB constructs a powerful ensemble of regression trees by iteratively minimizing a loss function using second-order gradient descent [45]. It introduces dropout regularization in the boosting process [46], which helps improve generalization, reduce overfitting, and lower both bias and variance. Unlike traditional implementations where XGB is used directly on input features, here it is utilized as a meta-model that operates on the prediction outputs of six diverse regressors: LSTM, ELM, SVM, ResNet, Bayesian Regression, and RNN. This integration allows the stacking model to benefit from both linear and nonlinear predictive behaviors present in the base models. The structure of the XGB algorithm is outlined in Fig. 8.

Within the stacking framework, XGB serves several key functions:

- *Leveraging Diverse Model Strengths* By aggregating predictions from multiple base models, the meta-model captures a richer set of patterns and reduces the likelihood of systemic bias.
- *Error Minimization* Prediction errors from base models are refined by the meta-model to produce a more accurate final output.

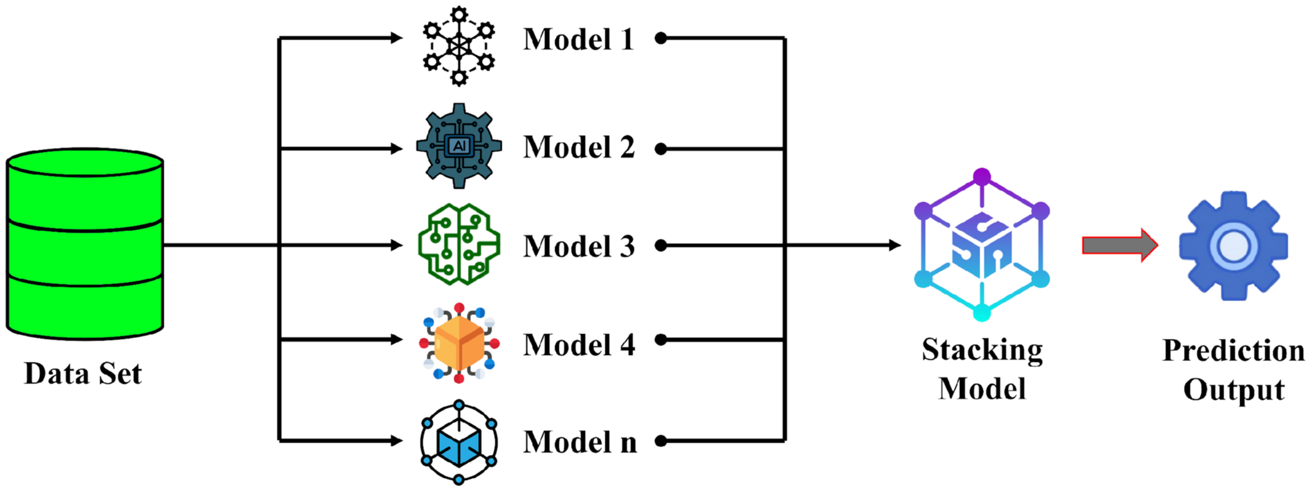


**Fig. 7** Workflow of the stacking-based regression model

**Fig. 8** Process diagram of the XGB algorithm

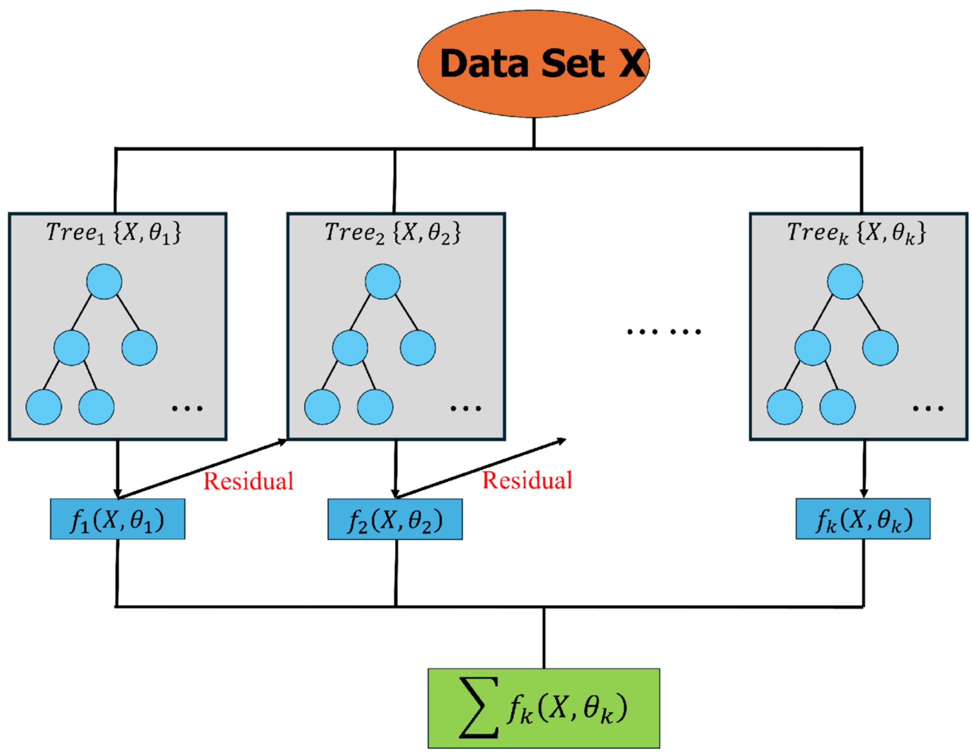


- *Hybrid Integration of Linear and Nonlinear Models* XGB enables the effective combination of fundamentally different modeling approaches within a single unified prediction pipeline.

The flexibility and scalability of XGB make it particularly well-suited for wave height prediction. Through hyperparameter tuning, the model's performance was further optimized, allowing for the selection of the most effective configuration based on experimental evaluation.

## 2.9 Evaluation metrics

To assess the accuracy and performance of the developed prediction models, four commonly used evaluation metrics were employed: Coefficient of Determination ($R^2$), Root Mean Square Error (RMSE), Mean Absolute Error (MAE), and Mean Square Error (MSE). These metrics provide insight into how closely the predicted values match the actual observations and quantify the magnitude of prediction errors. The mathematical formulations of these metrics are as follows:

$$R^2 = \left(1 - \frac{\sum_{t=1}^{N}(f_t - y_t)^2}{\sum_{t=1}^{N}(f_t - \overline{y})^2}\right) \tag{5}$$

$$\mathrm{RMSE} = \sqrt{\frac{\sum_t (f_t - y_t)^2}{N}} \tag{6}$$

$$\mathrm{MAE} = \frac{\sum_t |f_t - y_t|}{N} \tag{7}$$

$$\mathrm{MSE} = \frac{\sum_t (f_t - y_t)^2}{N} \tag{8}$$

where $f_t$ is the actual value, $y_t$ is the predicted value, $N$ is the number of predictions and $\overline{y}$ is the mean of the test values.

### 2.10 Wave energy estimation

Regular ocean waves consist of numerous small wave components, each with its own height, period, and direction of propagation. In real sea states, where many such components interact simultaneously, there is no single wave height or period. Instead, wave energy is typically characterized by using two parameters that are independent of wave direction: significant wave height $H_s$ (in meters) and wave period $T_e$ (in seconds). These spectral wave parameters are widely used to estimate the energy flux per meter of wave crest, expressed in watts per meter [12]. The wave power per unit wave crest length can be calculated using the following equation:

$$P = \frac{\rho . g^2}{64\pi} \times H_s^2 \times T_e \tag{9}$$

where $\rho$ is the density of sea water in kg/m$^3$, $g$ is the earth's gravity in m$^2$/sec, $H_s$ is significate wave height in m, and $T_e$ wave period in second. Some studies in the literature, for the Black Sea, assuming a seawater density of 1015 kg/m$^3$ [12], Eq. (9) can be simplified as follows:

$$P(\mathrm{kW/m}) = 0.486 \times H_s^2 \times T_e \tag{10}$$

This simplified formula was used to calculate the wave energy potential in the Black Sea region based on buoy data, serving as a basis for evaluating the accuracy of the machine learning-based prediction models.

In this study, the wave energy potential is estimated to be using an indirect approach based on the predicted wave height and wave period values. Compared to direct wave energy prediction, this strategy aims to reduce the adverse effects of measurement noise and rare high-energy wave events on the model performance. Consequently, the proposed framework provides more stable and reliable estimates, particularly for short- to medium-term energy forecasting, and offers a structure well-suited for real-time energy management applications.

## 3 Results and discussion

In this study, wave power potential was estimated by separately predicting significant wave height and wave period, which were then used in Eq. (9) to compute the final wave energy values. Rather than directly forecasting wave power, which can be sensitive to noise and uncertainties in raw buoy data—an indirect two-step strategy was adopted to minimize the influence of potentially distorted measurement parameters. To achieve this, six distinct regression models, i.e., LSTM, ELM, Bayesian, SVM, ResNet, and RNN were employed. Each model was independently trained and evaluated for both wave height and wave period predictions. The predictive performance of each approach was systematically compared using four statistical evaluation metrics: $R^2$, RMSE, MAE, and MSE. This multi-model, metric-based evaluation allowed for a comprehensive analysis of each algorithm's strengths and limitations in capturing the temporal dynamics of ocean wave behavior.

### 3.1 Ordu buoy

Wave height and period predictions based on data from the Ordu buoy reveal a clear trend across different forecasting horizons. As the prediction interval increases, a consistent deterioration in model performance is observed—characterized by rising RMSE, MAE, and MSE values, and a corresponding decline in $R^2$. This outcome highlights the increasing uncertainty associated with longer forecasting windows and suggests that the models face challenges in capturing the complex dynamics over extended timeframes.

Among the models evaluated, ResNet consistently outperformed all other regression approaches across all time intervals. Particularly in short-term predictions (1–6 h), ResNet demonstrated remarkable accuracy, yielding low error metrics alongside high $R^2$ scores. These results underscore the model's strength in learning short-term wave dynamics effectively.

ResNet's performance remained robust in mid-term forecasts as well. In 3-h predictions, it achieved excellent results with minimal errors and strong correlation. Although a slight degradation in performance was seen at 6 and 12 h intervals, the accuracy remained competitively high. Even at the 24 h mark, ResNet maintained its predictive reliability. However, in the 72-h forecasts, a notable increase in RMSE and MAE accompanied by a drop in $R^2$ suggests a limitation in long-term generalization capacity, likely due to the inherent complexity and noise in wave data.

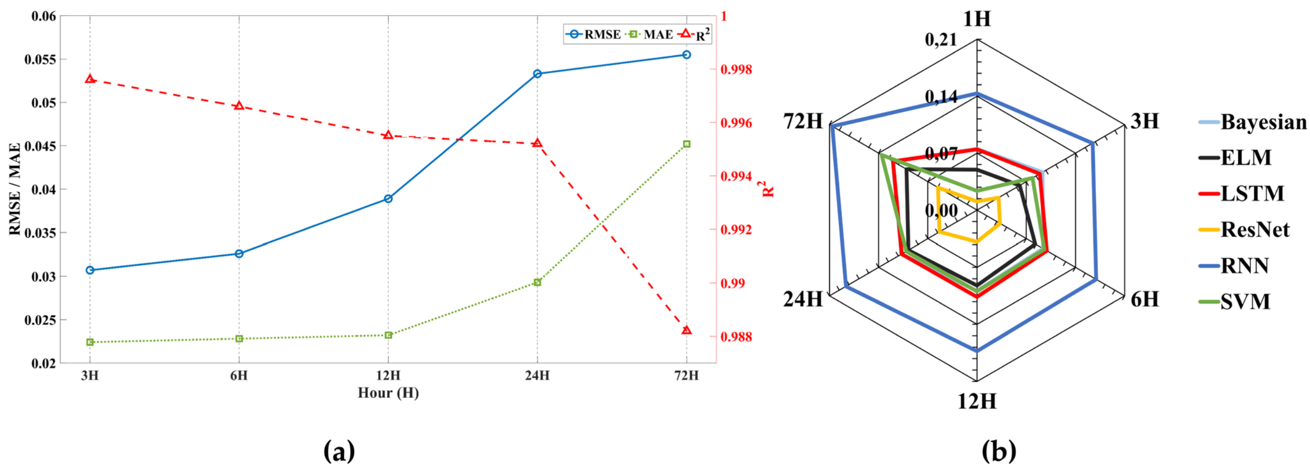


**Fig. 9** Wave height prediction for Ordu buoy **a** ResNet performance metrics over different time intervals, **b** RMSE comparison of all models for 24 h prediction

Beyond short-term accuracy, ResNet also demonstrated superiority in mid-range wave height prediction, suggesting its architecture can effectively capture temporally-evolving nonlinear patterns. The metric trends of ResNet across different time windows and the RMSE comparisons of all models for 24 h forecasts are presented in Fig. 9.

A similar pattern was observed in the prediction of wave period. Once again, ResNet showed the best overall performance, surpassing other models in all time horizons with lower error values and higher $R^2$ scores. The model exhibited strong predictive ability particularly in the 3–6 h range. While error metrics remained stable at 12 h, a sharper drop in correlation was noted. As the forecast horizon extended to 72 h, performance gradually declined, indicating the need for more complex input features or model architectures to handle long-term variability. ResNet's error and correlation trends, as well as comparative RMSE values across all models, are shown in Fig. 10.

Overall, ResNet clearly stands out among the regression models in both wave height and period forecasting tasks. While LSTM and RNN which are models typically well-suited for time series data, also performed reasonably well, they were more sensitive to fluctuations in the input parameters, which likely limited their effectiveness in capturing the complexity of wave behavior. ResNet's strength lies in its residual connections, which facilitate deeper learning without degradation—an advantage particularly useful in modeling the nonlinear and chaotic nature of ocean waves. In contrast, traditional models like Bayesian regression, SVM, and ELM achieved acceptable performance in short-term predictions, but their accuracy notably declined at longer intervals.

The RNN model consistently yielded the weakest results, especially in wave height prediction. It is worth noting, however, that for wave height, RMSE values among models were relatively close, indicating less variance in predictive capability. For wave period prediction, model RMSEs increased steadily with time, but the ranking of models by performance remained largely consistent. Notably, ResNet maintained its lead in all time intervals.

A deeper analysis of ResNet's metrics shows that wave height predictions began to deteriorate notably in error after the 12 h mark, with correlation declining beyond 24 h. For wave period, error metrics increased in a near-linear fashion, while a sharp drop in $R^2$ was again observed after 12 h. These trends suggest that while ResNet excels in capturing short- and medium-term dynamics, long-term forecasting remains a challenge due to rising input uncertainty and system complexity.

## 3.2 Samsun Buoy

Although the prediction performance of regression models based on the Samsun buoy data exhibits differences compared to the Ordu buoy, the general behavioral trends remain consistent. When examining model performance across various forecast horizons, a typical pattern emerges: As the time window extends, error metrics such as RMSE, MAE, and MSE increase, while the $R^2$ declines. Since the regression models were applied without modification across both buoys, observing similar trends is expected and supports the design goal of broad regional applicability. Notably, the hybrid model was intentionally developed without location-specific parameter tuning, to assess its generalization capability across different buoy datasets. However, as in the Ordu case, longer prediction intervals at the Samsun buoy resulted in increased uncertainty, challenging the models' ability to accurately represent wave dynamics over extended periods.

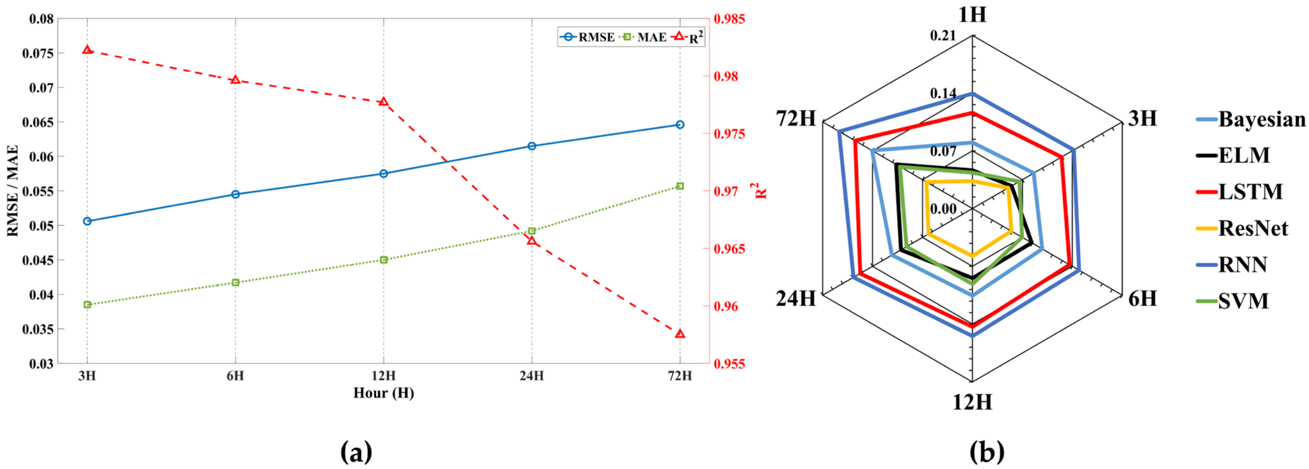


**Fig. 10** Wave period prediction for Ordu buoy, **a** ResNet performance metrics over different time intervals, **b** RMSE comparison of models across all time intervals

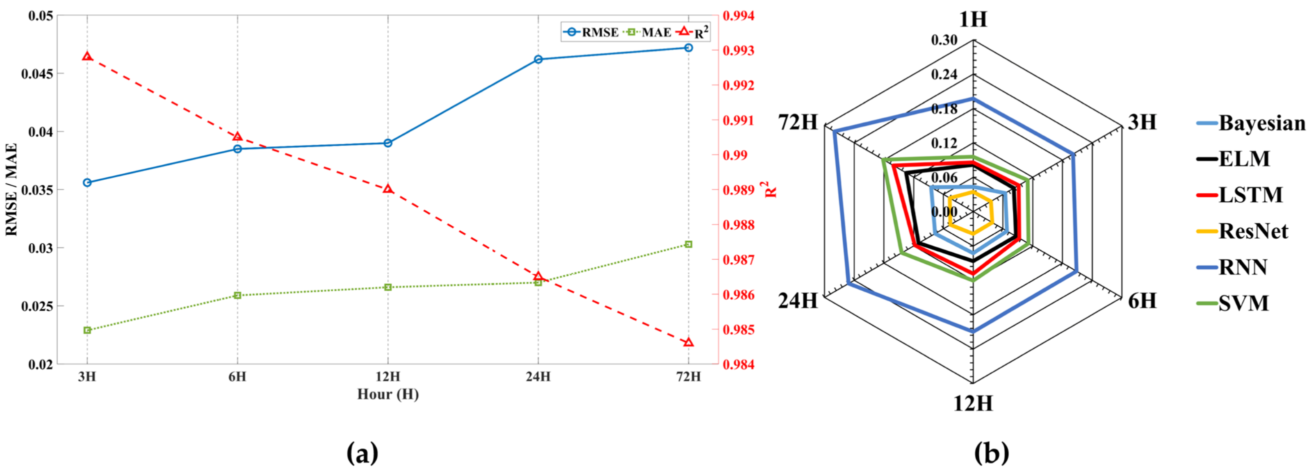


**Fig. 11** Wave height prediction results for Samsun buoy; **a** temporal variation of ResNet's performance metrics; **b** RMSE values for all models across all time windows

Among all models, ResNet consistently outperformed the others across all time frames. Particularly for short-term forecasts (1–6 h), it achieved notably low error rates and high $R^2$ values, highlighting its capacity to effectively capture short-term wave behavior. In the 3 h forecast scenario, ResNet maintained strong predictive accuracy with high correlation and minimal error. This performance trend continued with 6 and 12 h forecasts, with only minor increases in error. Even at the 24 h interval, ResNet sustained reliable results, although its accuracy began to decline. For the 72 h forecast, the model's error metrics rose significantly, and the $R^2$ score dropped, indicating that long-range predictions involve greater uncertainty, and that the model's robustness diminishes under such conditions. Regarding wave height predictions, ResNet again stood out by demonstrating a high level of predictability and generalizability across time frames. Figure 11a illustrates how its performance metrics evolved over time, while Fig. 11b compares RMSE values across all models and time intervals.

In wave period predictions, ResNet also achieved the best results, delivering the lowest error metrics and the highest $R^2$ scores across all forecast horizons. The correlation coefficient showed a generally linear decreasing trend with time, and performance degradation became especially evident in the 72 h predictions. The detailed evolution of ResNet's metrics for wave period prediction and comparative RMSE values across models are presented in Fig. 12.

Overall, the ResNet model demonstrated the highest prediction accuracy for both wave height and wave period based on the Samsun buoy data. In contrast, the RNN model showed the weakest performance, particularly in wave height prediction, where its MAE value was considerably higher than in wave period prediction. Unlike in the Ordu buoy case, the SVM model yielded higher error levels in wave height estimation for Samsun. While conventional models

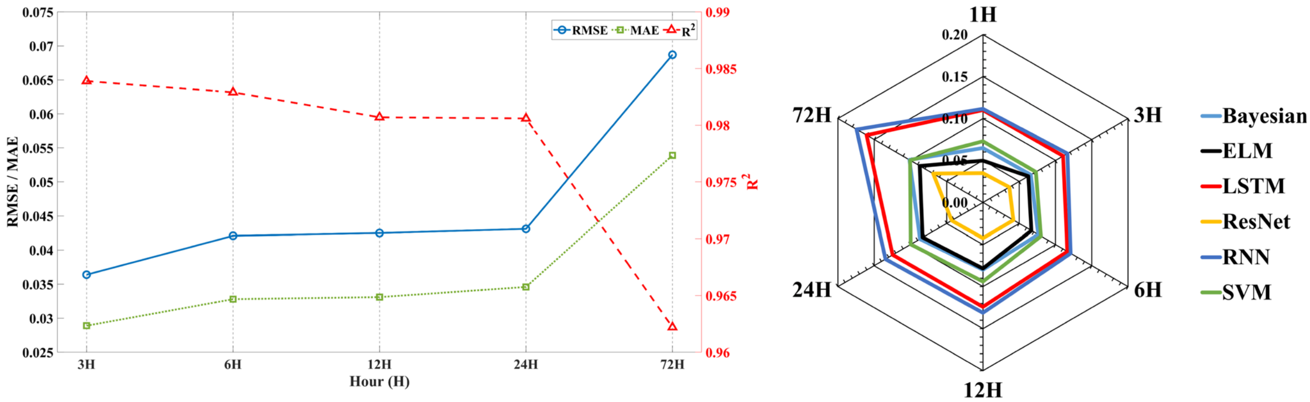


(a) (b)

**Fig. 12** Wave period prediction results for Samsun buoy; **a** temporal variation of ResNet's performance metrics; **b** RMSE values for all models across all time windows

like Bayesian, SVM, and ELM performed reasonably well in short-term predictions, their accuracy declined notably over longer horizons. Among all, RNN consistently ranked lowest in performance.

In the Samsun dataset, RMSE values for wave height prediction varied closely across the models, but this consistency did not extend to wave period prediction, where RMSE values increased more distinctly with time. Notably, the relative ranking of models remained largely stable, except for SVM and Bayesian models, whose performance metrics fluctuated closely enough to swap rankings occasionally at certain forecast intervals.

A detailed examination of ResNet's error and correlation metrics across time windows reveals that in wave height predictions, a sudden increase in error and a linear drop in correlation emerged after 24 h. For wave period forecasts, both error metrics and the correlation coefficient exhibited sharp deterioration beyond the 24 h mark. The model configurations, including parameters such as the number of hidden neurons and learning rates, were determined based on the Ordu buoy dataset. Notably, the Samsun buoy data featured a less complex distribution compared to Ordu, with fewer extreme values. These differences are likely attributable to the distinct environmental conditions and geographic characteristics of the two buoy locations. The similarity in model design across locations provided an opportunity to assess their adaptability and performance consistency. To further enhance wave power prediction across varying buoy datasets, a stacking-based ensemble model was developed by integrating different regression algorithms with complementary strengths. This hybrid model was trained and tested using data from both buoys without modifying the underlying parameters of individual algorithms. This approach was adopted to test the robustness and flexibility of the hybrid system in handling heterogeneous data characteristics. The successful deployment of this model across two geographically distinct locations suggests that it holds promise for broader application across the Black Sea region.

In summary, among the baseline regression models tested on data from both Samsun and Ordu buoys, ResNet consistently offered the most accurate and reliable predictions for both wave height and wave period. Its strong performance, especially for short- and mid-term forecasts, positions it as a suitable candidate for real-time wave energy prediction systems. However, the noticeable decline in accuracy over longer forecast periods underscores the potential value of hybrid or ensemble-based solutions in future work.

### 3.3 Stacking approaches

Wave height and period forecasts at the Ordu and Samsun buoys were conducted using six base regression models: Bayesian, ELM, LSTM, ResNet, RNN, and SVM. The predicted values generated by these base models were then used as inputs for the XGB algorithm in the stacking ensemble framework. The performance of the XGB algorithm within the stacking approach was benchmarked against the ResNet model, which served as a strong deep learning baseline.

For the Ordu buoy, the forecasting performances of the ResNet and XGB algorithms for both wave height and wave period are illustrated in Fig. 13. In the wave height prediction task, the RMSE, MAE, and MSE metrics followed a similar trend. For 1 h forecasts, ResNet outperformed XGB across all three metrics. However, for longer forecast horizons (3, 6, 12, 24, and 72 h), XGB showed better performance than ResNet in terms of RMSE, MAE, and MSE. Interestingly, ResNet consistently achieved higher $R^2$ values than XGB across all time intervals, indicating its superior ability to capture the variance in the data. When analyzing wave period predictions, XGB achieved better results than ResNet in terms of

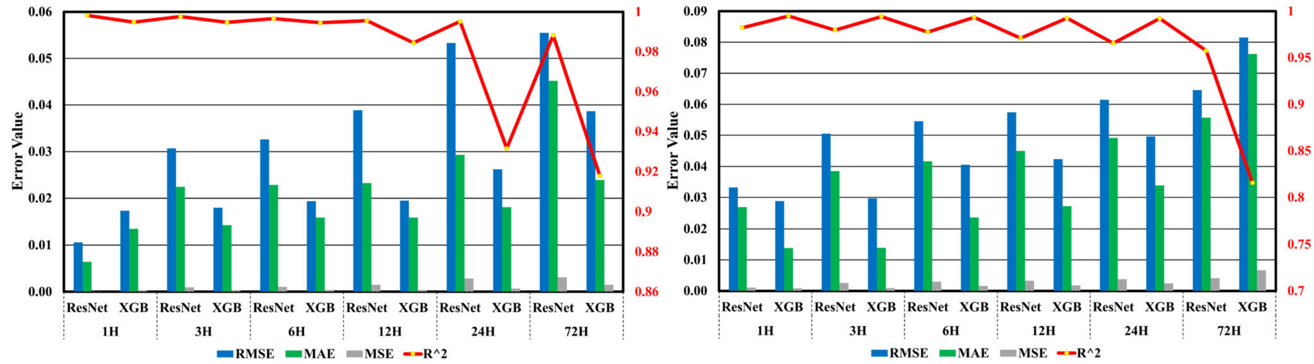


(a) (b)

**Fig. 13** Comparison of ResNet and XGB models for the Ordu buoy: **a** Wave height; **b** wave period

RMSE, MAE, $R^2$, and MSE across all time intervals except for the 72 h forecast. In that case, ResNet outperformed XGB.

Regarding wave height prediction at the Ordu buoy, ResNet outperformed XGB in all metrics for the 1 h forecast window. Additionally, ResNet achieved higher $R^2$ scores than XGB at every time step. This performance distribution can be explained by two key observations:

The XGB model used in the stacking approach was not directly trained on raw buoy data but on the outputs of the base regressors. For the 1 h horizon, the base models (excluding ResNet) performed suboptimally, which led to the XGB model being unable to correct these prediction errors effectively due to the limited sample size. In contrast, ResNet was trained directly on the original data and exhibited better accuracy and generalization in this short-term forecast scenario.

While RMSE, MAE, and MSE focus on the magnitude of prediction errors, the $R^2$ metric evaluates how well the model captures the variance and overall trend of the data. ResNet's superior $R^2$ values across all intervals suggest that it was more effective in recognizing underlying patterns. This can be attributed to ResNet's strong feature extraction and pattern-learning capabilities, while XGB is more sensitive to outliers and requires extensive hyperparameter tuning to achieve optimal performance.

In wave period prediction for the Ordu buoy, XGB surpassed ResNet in all metrics except for the 72 h forecast. This exception is largely due to a sharp performance drop in some of the base models, particularly RNN and LSTM, whose errors significantly increased at the 72 h horizon. These subpar outputs appear to have degraded the XGB model's overall performance, allowing ResNet to regain an advantage in that case. For the Samsun buoy, performance metrics of ResNet and XGB in forecasting wave height and period are presented in Fig. 14. The results show that the XGB model outperformed ResNet across all metrics and time intervals for both wave height and wave period.

An overall evaluation of the Samsun buoy forecasts reveals that XGB consistently outperformed ResNet across all time intervals and performance metrics. One possible explanation is that the Samsun buoy data exhibits smoother transitions and less variability compared to the Ordu buoy data. This smoother dataset enables the stacking-based XGB model to minimize prediction errors more effectively, resulting in superior performance across both tasks.

## 3.4 Wave power estimation based on predicted parameters

The primary objective of the proposed system is to estimate wave power using buoy data. To achieve this, wave height and wave period are predicted separately. The predicted wave power is calculated using the estimated wave height and period values as defined in Eq. (11):

$$P_{\text{pred}}(\text{kW/m}) = 0.486 \times H_{\text{pred}}^2 \times T_{\text{pred}} \tag{11}$$

Similarly, the actual wave power is calculated from buoy-measured wave height and period using Eq. (12):

$$P_{\text{test}}(\text{kW/m}) = 0.486 \times H_{\text{test}}^2 \times T_{\text{test}} \tag{12}$$

To evaluate the effectiveness of the stacking approach, performance metrics of the XGB and ResNet models were compared for wave power predictions. Figure 15 illustrates the predicted and test wave power values over a 6-h period at the Ordu buoy using both XGB and ResNet algorithms. Sudden surges in wave power caused higher discrepancies between predicted and actual values, highlighting the difficulty of accurately estimating wave power during rare high-energy events. These anomalies are harder for ML models to capture due to their infrequency in the training data. Similarly, Fig. 16 shows the comparison between predicted

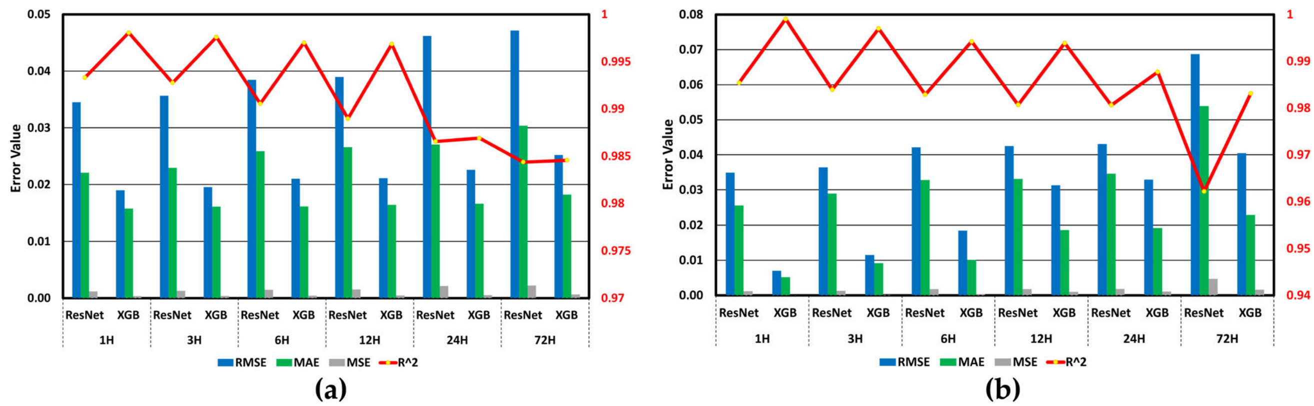


**Fig. 14** Comparison of ResNet and XGB models for the Samsun buoy: **a** Wave height; **b** wave period

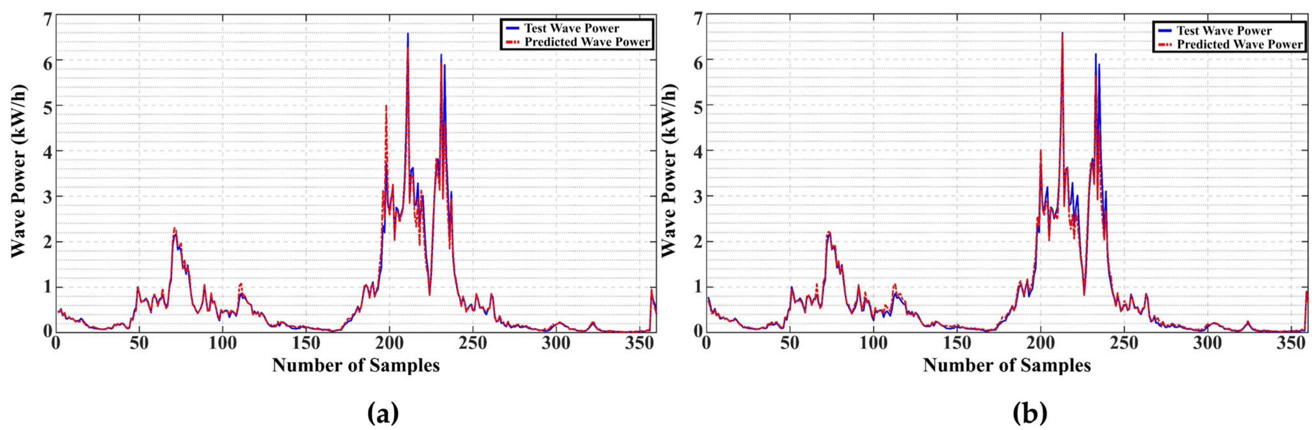


**Fig. 15** **a** XGB-predicted vs. test wave power at Ordu buoy; **b** ResNet-predicted versus test wave power at Ordu buoy

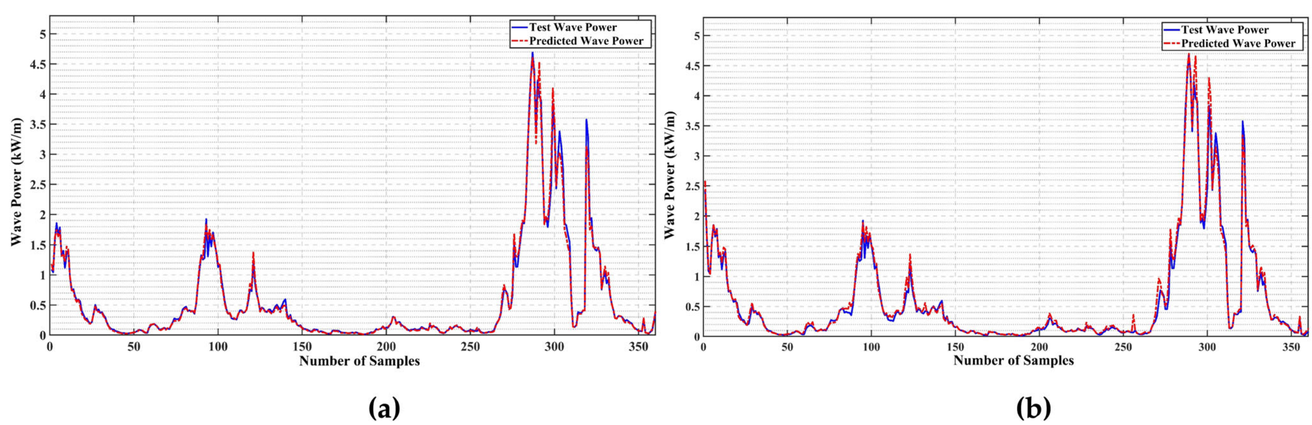


**Fig. 16** **a** XGB-predicted vs. test wave power at Samsun buoy; **b** ResNet-predicted vs. test wave power at Samsun buoy

and actual wave power values at the Samsun buoy. It is evident that the XGB algorithm provides results closely aligned with actual values across all time intervals.

The performance metrics for both models in predicting wave power across Ordu and Samsun buoys are presented in Fig. 17. For the Ordu buoy, RMSE and MSE values are similar for both models in 1 h predictions, but XGB outperforms ResNet in other time intervals. In terms of MAE and $R^2$, XGB consistently shows better performance. At the Samsun buoy, the XGB model outperforms ResNet across all performance metrics and time intervals.

Direct wave power estimation from buoy data could be an alternative approach. However, wave height and wave period are influenced by different environmental factors. Thus, estimating them separately improves accuracy. Direct

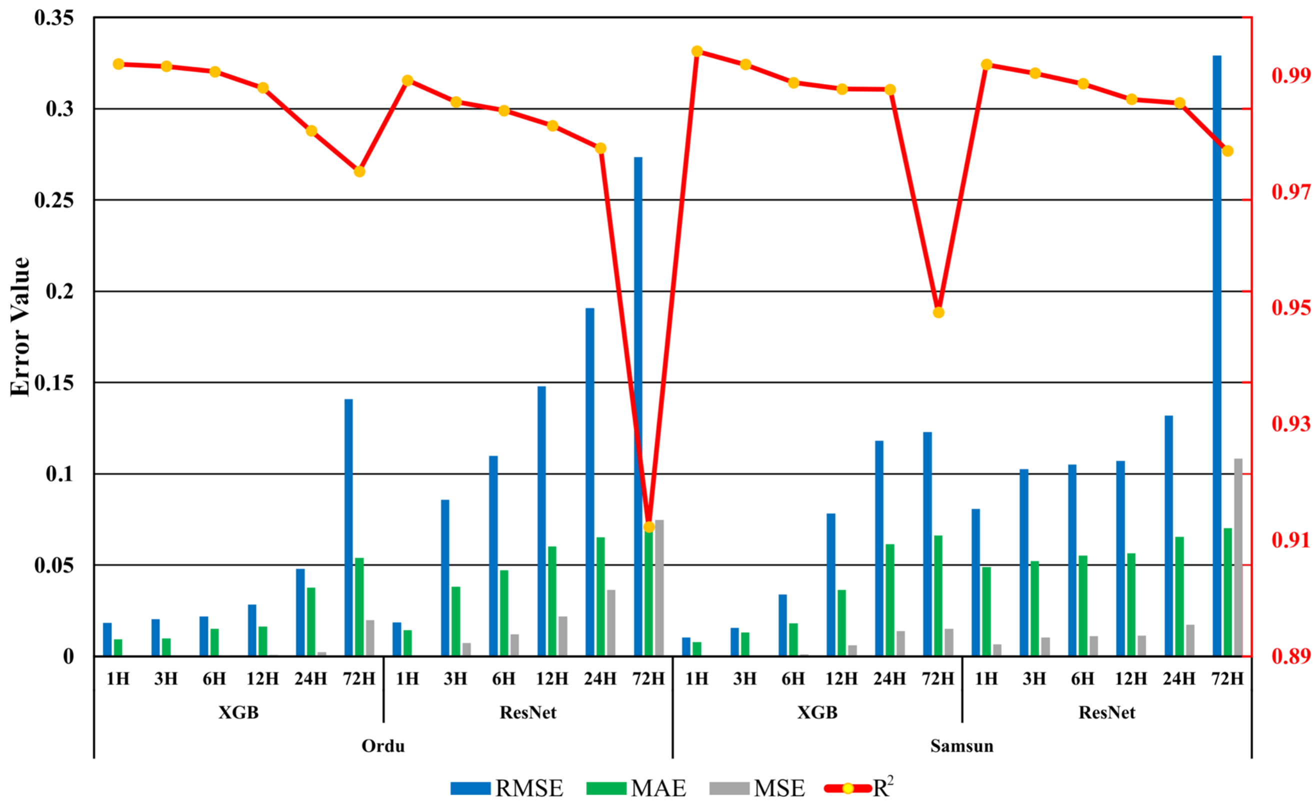


**Fig. 17** Comparison of RMSE, MAE, MSE, and $R^2$ values for ResNet and XGB models at different forecasting horizons for both buoy stations

prediction of wave power would likely increases error values and reduces the effectiveness of the stacking approach.

## 3.5 Model performance comparison

Wave power prediction performance was further analyzed for both ResNet and XGB models. Overall, the XGB model exhibited superior prediction accuracy at both buoy locations. At the Samsun buoy, XGB significantly outperformed ResNet. At the Ordu buoy, XGB again yielded slightly better results, with smaller performance gaps. The differences between the two buoys are attributed to the base regression models used to predict wave height and period, which vary in performance based on the buoy location and environmental features.

Although XGB demonstrated strong results, it is important to note that it operates as a meta-model in a stacking ensemble. Its input is the output of six base regression models. By leveraging the strengths of these models, XGB effectively reduces overall error and increases $R^2$ scores especially in short-term forecasts. Despite increased uncertainty in long-term predictions, XGB still surpasses individual base models in performance. Performance comparisons among base models revealed the following:

- *LSTM and RNN:* Effective at capturing temporal dependencies but yielded lower overall accuracy. Particularly underperformed in short-term (1H, 3H) forecasts.
- *SVM and ELM:* Performed reasonably well on small datasets but struggled with nonlinear and complex buoy data.
- *ResNet:* Delivered the best accuracy among base models, especially for mid-range forecasts (6H, 12H), but its accuracy declined with longer horizons.
- *Bayesian Regression:* Advantageous for modeling uncertainty yet limited in deterministic accuracy.

Each model has specific strengths and weaknesses:

- *LSTM:* Excellent for temporal modeling but prone to overfitting in deep configurations.
- *ELM:* Offers rapid results even on large datasets but lacks generalization compared to LSTM/ResNet.
- *SVM:* Effective for nonlinear relationships but requires careful hyperparameter tuning.
- *ResNet:* Well-suited for capturing complex, long-term patterns but requires significant training time and data.
- *Bayesian:* Captures probabilistic uncertainty but is computationally intensive.
- *RNN:* Good for sequence modeling but weak in handling long-term dependencies.

Given these characteristics, ResNet was expected to outperform other base models, which it generally did. However, the XGB model by integrating outputs from all base models ultimately achieved the highest performance in wave power estimation. The superiority of the XGB model was more pronounced in Samsun than in Ordu. The results reflect the regional variability in buoy data quality and the interaction of prediction features. At both locations, XGB performed strongly in short-term forecasts, while ResNet lagged behind overall.

The difference in feature sets for wave height and period prediction also influenced model performance. Some depth current parameters used for wave height prediction negatively impacted period prediction, so they were excluded. Studies by Karabulut and Ozmen [26] demonstrated the relevance of 5 m, 10 m, and 15 m depth currents in wave height prediction. Their findings confirmed that combining all three depths improved accuracy but also increased computational time—a similar outcome observed in this study.

In the context of the Black Sea, most previous studies like Akpınar et al. [47], Islek et al. [48], and Rusu [49] have utilized physical models such as SWAN and to estimate wave power. However, no study in the literature has used real buoy data and machine learning methods to directly estimate the wave power and energy potential of specific locations within the Black Sea.

Key differences between this approach and SWAN-based studies include:

- *Modeling method:* SWAN uses physical equations and wind data to simulate wave dynamics; this study uses ML to predict wave parameters directly from measured data.
- *Application scope:* SWAN is commonly used for large-scale coastal engineering; this study targets real-time, location-specific energy generation potential.
- *Forecast granularity:* SWAN focuses on long-term power trends; this study enables short-term and near-real-time forecasting.
- *Spatial resolution:* SWAN models broad regions; this study offers high-resolution analysis for specific sites (Samsun and Ordu).

In conclusion, the stacking approach incorporating the XGB algorithm significantly enhances the accuracy of wave power prediction based on real-time buoy data. This method offers a promising alternative to traditional physical modeling, particularly for localized, real-time energy forecasting applications.

### 3.6 Comparison with literature

The wave height prediction results obtained in this study were compared with similar studies conducted in different regions and over various forecasting horizons reported in the literature. Since the datasets, geographical locations, and modeling approaches differ among studies, a direct one-to-one comparison is not feasible. Nevertheless, comparing the order of magnitude of commonly used error metrics, such as RMSE and $R^2$, provides a meaningful basis for evaluating predictive performance. In the study conducted by Fan et al. [50], RMSE values for wave height prediction were reported to range between 0.07 and 0.32 m. Similarly, PMR Bento et al. [11] reported RMSE values in the range of 0.3–0.5 m, while Mousavi et al. [28] obtained RMSE values between 0.49 and 0.56 m for wave height forecasting. Compared with these studies, the proposed method demonstrates RMSE values that are within the reported ranges and, in several short- and medium-term forecasting cases, achieves lower prediction errors.

Considering the influence of regional characteristics on prediction performance, Karabulut [26] reported RMSE values of 0.064–0.074 m and $R^2$ values ranging from 0.85 to 0.95 using Mediterranean Sea data. In the analysis performed by Sadeghifar et al. [27] for different forecasting horizons, RMSE values of 0.39, 0.44, 0.38, and 0.32 m were reported for 3, 6, 12, and 24 h prediction intervals, respectively, while the corresponding $R^2$ values exhibited a decreasing trend from 0.96 to 0.80. These findings indicate that prediction performance naturally degrades as the forecasting horizon increases, which is consistent with the trends observed in the present study. In the work of Yao et al. [17], conducted using data from the Hong Kong coastline, wave height predictions over time horizons ranging from 0.5 to 12 h yielded RMSE values between 0.11 and 0.79 m and $R^2$ values between 0.89 and 0.99. This wide performance range highlights the strong influence of both forecasting horizon and regional wave regimes on prediction accuracy.

Overall, the machine learning-based stacking approach presented in this study exhibits performance levels that are consistent with those reported in the literature across different geographical regions and forecasting horizons. In particular, the RMSE and $R^2$ values achieved for short- to medium-term forecasts demonstrate that the proposed method provides a reliable and competitive alternative for wave height prediction. Moreover, this Black Sea-focused study offers a quantitative contribution to the limited number of data-driven wave forecasting studies available for this region, highlighting the adaptability of the proposed framework to regional wave conditions.

## 4 Conclusion and future works

This study introduced an operational, data-driven framework for forecasting wave energy potential in the Black Sea, specifically utilizing high-resolution buoy observations from

Samsun and Ordu. By implementing a stacking ensemble architecture that employs XGB as a meta-learner to synthesize predictions from six diverse regressors (LSTM, ELM, SVM, Bayesian Regression, ResNet, and RNN), the proposed approach significantly enhanced prediction accuracy across all standard metrics. Our findings demonstrate that this ensemble strategy consistently outperforms individual models, providing a more robust solution for handling the nonlinear dynamics of marine environments.

The quantitative comparison between the ensemble framework and the ResNet baseline revealed substantial performance gains. At the Ordu station, the XGB-based ensemble achieved a dramatic 75% reduction in RMSE for 24 h ahead forecasts—dropping from 0.1908 to 0.0481—and maintained a 50% lower error rate even at the 72 h horizon. The results at the Samsun station were similarly impressive, particularly for short-term forecasts where the 1 h ahead RMSE showed an improvement of over 85% compared to individual models. Despite the inherent degradation in accuracy as the forecasting window expands, the framework remained remarkably stable, maintaining $R^2$ values as high as 0.9735 at the 72 h mark. From a regional perspective, the framework effectively adapted to the distinct wave dynamics of each location, with the Samsun buoy yielding slightly more consistent results due to its smoother data distribution. Unlike traditional physics-based models that require heavy computational resources and external meteorological inputs, our method offers a faster, site-specific alternative for real-time energy management and operational decision-making in the Black Sea. This research fills a critical gap in regional literature as one of the first applications of ensemble learning on actual buoy data for wave power estimation in this basin.

While the current framework excels in short- to medium-term forecasting, future work will aim to extend these predictions to seasonal and long-term horizons by integrating multi-year datasets and large-scale climate variables. Furthermore, we plan to explore hybrid models that combine physics-based equations with machine learning to better capture rare, high-energy wave events. Expanding this framework to other coastal sites and developing a real-time, user-accessible forecasting tool could significantly benefit the planning and grid integration of wave energy converter systems in the region.

**Funding** Open access funding provided by the Scientific and Technological Research Council of Türkiye (TÜBİTAK).

**Data Availability** Data included in article/supp. material/referenced in article.

## Declarations

**Conflict of ınterest** The authors declare no conflict of interest.



## References

1. R. Revelle, Requirements for energy in the rural areas of developing countries. In: Renewable Energy Resources and Rural Applications in the Developing Wo, pp. 11–26. Routledge (2019)
2. D.J. Soeder; D.J. Soeder, Fossil fuels and climate change, Fracking and the Environment: A Scientific Assessment of the Environme Risks from Hydraulic Fracturing and Fossil Fuels, pp. 155–185 (2021)
3. Al-Shetwi, A.Q.: Sustainable development of renewable energy integrated power sector: t rends, environmental impacts, and recent challenges. Sci. Total. Environ. **822**, 153645 (2022)
4. Zayed, M.E.; Kabeel, A.E.; Shboul, B.; Ashraf, W.M.; Ghazy, M.; Irshad, K.; Rehman, S.; Zayed, A.A.A.: Performance augmentation and machine learning-based modeling of wavy corrugated solar air collector embedded with thermal energy storage: Support vector machine combined with Monte Carlo simulation. J. Energy Storage **74**, 109533 (2023). https://doi.org/10.1016/j.est.2023.109533
5. Mohandes, M.A.; Halawani, T.O.; Rehman, S.; Hussain, A.A.: Support vector machines for wind speed prediction. Renew. Energy **29**, 939–947 (2004). https://doi.org/10.1016/j.renene.2003.11.009
6. Lawal, A.; Rehman, S.; Alhems, L.M.; Alam, M.M.: Wind speed prediction using hybrid 1D CNN and BLSTM network. IEEE Access **9**, 156672–156679 (2021). https://doi.org/10.1109/ACCESS.2021.3129883
7. Reikard, G.; Robertson, B.; Bidlot, J.-R.: Combining wave energy with wind and solar: short-term forecasting. Renew. Energy **81**, 442–456 (2015)
8. Jeon, J.; Taylor, J.W.: Short-term density forecasting of wave energy using ARMA-GARCH models and kernel density estimation. Int. J. Forecast. **32**, 991–1004 (2016)
9. Curto, D.; Franzitta, V.; Guercio, A.: Sea wave energy. A review of the current technologies and perspectives. Energies **14**, 6604 (2021)
10. Uihlein, A.; Magagna, D.: Wave and tidal current energy–a review of the current state of researc h beyond technology. Renew. Sustain. Energy Rev. **58**, 1070–1081 (2016)
11. Bento, P.M.R.; Pombo, J.A.N.; Mendes, R.P.G.; Calado, M.R.A.; Mariano, S.J.P.S.: Ocean wave energy forecasting using optimised deep learning neural net works. Ocean Eng. **219**, 108372 (2021). https://doi.org/10.1016/j.oceaneng.2020.108372
12. Akpınar, A.; Kömürcü, M.İ: Wave energy potential along the south-east coasts of the Black Sea. Energy **42**, 289–302 (2012)
13. Gorrell, L.; Raubenheimer, B.; Elgar, S.; Guza, R.T.: SWAN predictions of waves observed in shallow water onshore of complex bathymetry. Coast. Eng. **58**, 510–516 (2011)
14. Son, B.; Do, K.: Optimization of SWAN wave model to improve the accuracy of winter stor m wave prediction in the East Sea. J. Ocean Eng. Technol. **35**, 273–286 (2021)
15. Yang, S.; Zhang, Z.; Fan, L.; Xia, T.; Duan, S.; Zheng, C.; Li, X.; Li, H.: Long-term prediction of significant wave height based on

SARIMA model in the South China Sea and adjacent waters. IEEE Access **7**, 88082–88092 (2019). https://doi.org/10.1109/ACCESS.2019.2925107
16. Tarwidi, D.; Pudjaprasetya, S.R.; Adytia, D.; Apri, M.: An optimized XGBoost-based machine learning method for predicting wave run-up on a sloping beach. MethodsX **10**, 102119 (2023). https://doi.org/10.1016/j.mex.2023.102119
17. Yao, J.; Wu, W.: Wave height forecast method with multi-step training set extension LST M neural network. Ocean Eng. **263**, 112432 (2022). https://doi.org/10.1016/j.oceaneng.2022.112432
18. Anggraeni, F.; Adytia, D.; Ramadhan, A.W.: Forecasting of Wave Height Time Series Using AdaBoost and XGBoost. Case Study in Pangandaran, Indonesia, pp. 97–101. https://doi.org/10.1109/ICoDSA53588.2021.9617524
19. Teixeira-Duarte, F.; Clemente, D.; Giannini, G.; Rosa-Santos, P.; Taveira-Pinto, F.: Review on layout optimization strategies of offshore parks for wave en ergy converters. Renew. Sustain. Energy Rev. **163**, 112513 (2022)
20. Bas, B.; Gervásio, H.; Borg, R.P.; Tesch, L.; Musarat, M.A.; Jiang, X.: Life cycle assessment of marine renewable energy systems: a literature review for environmental sustainability assessment of floating modular energy islands (FMEIs). IOP Conf. Ser. Earth Environ. Sci. **1552**, 12039 (2025). https://doi.org/10.1088/1755-1315/1552/1/012039
21. Özhan, E.; Abdalla, S.: Türkiye kıyıları rüzgar ve derin deniz dalga atlası, MEDCOAST, ODTÜ (2002)
22. Sağlam, M.; Sulukan, E.; Uyar, T.S.: Wave energy and technical potential of Turkey. J. Nav. Sci. Eng. **6**, 34–50 (2010)
23. Yesilyurt, M.K., Öner, İ.V., Ömeroğlu, G., Yilmaz, E.Ç.: A scrutiny study on wave energy potential and policy in Turkey. In: Periodicals of Engineering and Natural Sciences (PEN) 5 (2017).
24. Abed-Elmdoust, A.; Kerachian, R.: Wave height prediction using the rough set theory. Ocean Eng. **54**, 244–250 (2012). https://doi.org/10.1016/j.oceaneng.2012.07.020
25. Zayed, M.E.; Rehman, S.; Elgendy, I.A.; Al-Shaikhi, A.; Mohandes, M.A.; Irshad, K.; Abdelrazik, A.S.; Alam, M.A.: Benchmarking reinforcement learning and prototyping development of floating solar power system: Experimental study and LSTM modeling combined with brown-bear optimization algorithm. Energy Convers. Manag. **332**, 119696 (2025). https://doi.org/10.1016/j.enconman.2025.119696
26. Karabulut, N.; Ozmen Koca, G.: Wave height prediction with single input parameter by using regression methods. Energy Sources A **42**, 2972–2989 (2020). https://doi.org/10.1080/15567036.2020.1733711
27. Sadeghifar, T.; Nouri Motlagh, M.; Torabi Azad, M.; Mohammad Mahdizadeh, M.: Coastal wave height prediction using recurrent neural networks (RNNs) in the south Caspian Sea. Mar. Geod. **40**, 454–465 (2017)
28. Mousavi, S.M.; Ghasemi, M.; Dehghan Manshadi, M.; Mosavi, A.: Deep learning for wave energy converter modeling using long short-term memory. Mathematics **9**, 871 (2021)
29. Hu, H.; Westhuysen, A.J.; Chu, P.; Fujisaki-Manome, A.: Predicting Lake Erie wave heights and periods using XGBoost and LSTM. Ocean Model **164**, 101832 (2021). https://doi.org/10.1016/j.ocemod.2021.101832
30. Huang, G.-B.; Zhu, Q.-Y.; Siew, C.-K.: Extreme Learning Machine: A New Learning Scheme of Feedforward Neural Networks, vol. 2, pp. 985–990 (2004). https://doi.org/10.1109/IJCNN.2004.1380068.
31. Moe, S.J.; Wolf, R.; Xie, L.; Landis, W.G.; Kotamäki, N.; Tollefsen, K.E.: Quantification of an adverse outcome pathway network by Bayesian regre ssion and Bayesian network modeling. Integr. Environ. Assess. Manag. **17**, 147–164 (2021). https://doi.org/10.1002/ieam.4348
32. Jones, A.M.; Lomas, J.; Moore, P.T.; Rice, N.: A Quasi-Monte-Carlo comparison of parametric and semiparametric regre ssion methods for heavy-tailed and non-normal data: an application to h ealthcare costs. J. R. Stat. Soc. A. Stat. Soc. **179**, 951–974 (2016). https://doi.org/10.1111/rssa.12141
33. Hochreiter, S.; Schmidhuber, J.: Long short-term memory. Neural Comput. **9**, 1735–1780 (1997). https://doi.org/10.1162/neco.1997.9.8.1735
34. Graves, A.: Long Short-Term Memory. In: Graves, A. (Ed.) Supervised sequence labelling with recurrent neural networks, pp. 37–45. Springer Berlin Heidelberg, Berlin, Heidelberg (2012). https://doi.org/10.1007/978-3-642-24797-2_4
35. Aljhohani, H.; Alshamrani, S.; Aljoj, N.; Tashkandi, A.; Alshafi, T.: Predicting monthly gold prices in Indian rupees using ARIMA, LSTM, GRU, and simple linear regression models. Rom. J. Inf. Technol. Autom. Control **34**, 35–48 (2024)
36. Mahdavi-Meymand, A.; Sulisz, W.: Application of nested artificial neural network for the prediction of significant wave height. Renew. Energy **209**, 157–168 (2023). https://doi.org/10.1016/j.renene.2023.03.118
37. Vapnik, V.: The Nature of Statistical Learning Theory. Springer-Verlag, New York (1995)
38. Smola, A.J.; Schölkopf, B.: A tutorial on support vector regression. Stat. Comput. **14**, 199–222 (2004)
39. Müller, K.-R.; Smola, A.J.; Rätsch, G.; Schölkopf, B.; Kohlmorgen, J.; Vapnik, V.: Using support vector machines for time series prediction. In: Advances in Kernel Methods: Support Vector Learning. The MIT Press (1998)
40. Ghafoorian, M.; Karssemeijer, N.; Heskes, T.; Bergkamp, M.; Wissink, J.; Obels, J.; Keizer, K.; Leeuw, F.-E.; Van Ginneken, B.; Marchiori, E.: Deep multi-scale location-aware 3D convolutional neural networks for a utomated detection of lacunes of presumed vascular origin. Neuroimage Clin. **14**, 391–399 (2017)
41. Bodhwani, V.; Acharjya, D.P.; Bodhwani, U.: Deep residual networks for plant identification. Proced. Comput. Sci. **152**, 186–194 (2019)
42. Lathuilière, S.; Mesejo, P.; Alameda-Pineda, X.; Horaud, R.: A comprehensive analysis of deep regression. IEEE Trans. Pattern Anal. Mach. Intell. **42**, 2065–2081 (2019)
43. Hajihosseinlou, M.; Maghsoudi, A.; Ghezelbash, R.: Stacking: A novel data-driven ensemble machine learning strategy for p rediction and mapping of Pb-Zn prospectivity in Varcheh district, west Iran. Expert Syst. Appl. **237**, 121668 (2024). https://doi.org/10.1016/j.eswa.2023.121668
44. Meharie, M.G.; Mengesha, W.J.; Gariy, Z.A.; Mutuku, R.N.N.: Application of stacking ensemble machine learning algorithm in predict ing the cost of highway construction projects. Eng. Constr. Archit. Manag. **29**, 2836–2853 (2022)
45. Massaoudi, M.; Refaat, S.S.; Chihi, I.; Trabelsi, M.; Oueslati, F.S.; Abu-Rub, H.: A novel stacked generalization ensemble-based hybrid LGBM-XGB-MLP mode l for short-term load forecasting. Energy **214**, 118874 (2021). https://doi.org/10.1016/j.energy.2020.118874
46. Vinayak, R.K.; Gilad-Bachrach, R.: Dart: Dropouts meet multiple additive regression trees. İn: PMLR, pp. 489–497 (2015)
47. Akpınar, A.; Bingölbali, B.; Van Vledder, G.P.: Long-term analysis of wave power potential in the Black Sea, based on. Ocean Eng. **130**, 482–497 (2017)
48. Islek, F.; Yuksel, Y.; Sahin, C.; Guner, H.A.A.: Long-term analysis of extreme wave characteristics based on the SWAN h indcasts over the Black Sea using two different wind fields. Dyn. Atmos. Oceans **94**, 101165 (2021)
49. Rusu, L.: A projection of the expected wave power in the Black Sea until the end of the 21st century. Renew. Energy **160**, 136–147 (2020)

50. Fan, S.; Xiao, N.; Dong, S.: A novel model to predict significant wave height based on long short-t erm memory network. Ocean Eng. **205**, 107298 (2020). https://doi.org/10.1016/j.oceaneng.2020.107298